SOME RESULTS ON THE ACCURACY OF AN EDGE-BASED FINITE VOLUME FORMULATION FOR THE SOLUTION OF ELLIPTIC PROBLEMS IN HETEROGENEOUS AND ANISOTROPIC POROUS MEDIA

Carvalho, D. K. E., dkarlo@uol.com.br
Núcleo de Tecnologia - Centro Acadêmico do Agreste (CAA)
Universidade Federal de Pernambuco (UFPE)
Rodovia BR 104, KM 62, S/N, Pólo Comercial Nova Caruaru,
Caruaru-PE, Brasil, CEP: 55002-970

Luna, B. G. B.[1], Willmersdorf, R. B.[2], Lyra, P. R. M.[3]
[1]bruno_bl@yahoo.com.br,[2]ramiro@willmersdorf.net,[3]prmlyra@ufpe.br

Departamento de Engenharia Mecânica (DEMEC)
Centro de Tecnologia e Geociências (CTG)
Universidade Federal de Pernambuco (UFPE)
Av. Acadêmico Hélio Ramos S/N Cidade Universitária, Recife – PE, Brasil, CEP: 50.740-470

Soares, R. S., rogsoares@yahoo.com.br
Departamento de Engenharia Civil (DECIV)
Centro de Tecnologia e Geociências (CTG)
Universidade Federal de Pernambuco (UFPE)
Av. Acadêmico Hélio Ramos S/N Cidade Universitária, Recife – PE, Brasil, CEP: 50.740-470

Abstract. *The modeling and simulation of fluid flow problems in heterogeneous and anisotropic porous media represents a great challenge from mathematical and numerical point of views. Particularly, the simulation of oil recovery in petroleum reservoirs, may involve the numerical solution of an elliptic type equation with highly discontinuous coefficients for the pressure field, and a non-linear hyperbolic type equation for the saturation field. In the present work, we present a node-centered finite volume method, with median dual control volumes using an edge-based data structure (EFVM). This formulation is capable of handling both, heterogeneous and anisotropic (full tensor) porous media using structured and unstructured meshes. The algorithm consists in a modification of the two step Crumpton's edge-based approach, which includes the cross-diffusion terms in an very ellegant manner. This formulation formally guarantees local conservation even for non-orthogonal meshes and highly discontinuous coeficients, keeping second order accuracy for the pressure field and, at least, first order accuracy for the velocity field on general triangular meshes. In order to verify the accuracy of the proposed edge-based finite volume procedure we present some numerical experiments involving heterogeneous and highly anisotropic materials. For the examples analyzed, numerical results compare very favorably with others found in literature.*

Keywords*: finite volume, edge-based, pressure equation, heterogeneous and anisotropic porous media*

1. INTRODUCTION

The task of modeling and simulating diffusion type problems in heterogeneous and anisotropic media can be a great challenge from a mathematical and numerical point of view. Abrupt variations in the permeability field (i.e. the diffusion coefficient) is a common feature whenever modeling and simulating fluid flow in petroleum reservoirs and aquifers. Over the last years, much effort has been put in developing numerical methods that make use of unstructured meshes, such as the finite element method (FEM) and the finite volume method (FVM), due the fact that these methods allow for better modeling of complex geometrical features and because they can easily incorporate mesh adaptive procedures. When handling conservation laws, FVM are particularly attractive as they conserve mass, globally and locally. It is well known that traditional "five point" finite difference methods (FDM) are unable to handle full tensors or non-orthogonal meshes. Besides, it can be proved that these schemes introduce first order errors in the approximation of flux terms between discontinuous materials (Edwards and Rogers, 1998), making these methods unsuitable for the modeling and simulation of fluid flow in highly heterogeneous and anisotropic porous media.

Locally conservative schemes, such as the mixed finite element method (MFEM) and flux continuous finite volumes (FCFV), also called multipoint flux approximations (MPFA), have been extensively studied in literature (Ewing, 1983; Aavatsmark *et al*, 1998, Edwards and Rogers, 1998; Edwards, 2000; Klausen and Eigestad, 2004). In the context of reservoir simulation, the recently developed FCFV are defined by assuming continuous pressures and normal fluxes across control volumes interfaces (Aavatsmark *et al*, 1998, Edwards and Rogers, 1998). Despite of the high computational costs associated to these methods, particularly the MFEM, both methods are capable of handling full tensors elliptic equations in highly non-homogeneous porous media using structured or unstructured meshes. The finite element method, which is globally, but not locally conservative (i.e. at element level), requires some kind of flux recovery in order to formally guarantee local conservation (Loula *et al*, 1999).

In the present paper, we show a node centered finite volume formulation in which median dual control volumes (Donald's dual) are used with an edge-based data structure (Luo *et al*, 1995; Crumpton *et al*, 1997; Rees *et al*, 2004; Carvalho *et al*, 2005) in such a way that the geometrical coefficients are associated to the edges and nodes of the primal mesh. This formulation, which is capable of handling structured or unstructured meshes, and non-homogeneous and anisotropic porous media, has been chosen due to the fact that vertex-centered FV schemes are usually superior to cell centered schemes in terms of memory usage (Luo *et al*, 1995; Rees *et al*, 2004), and because edge-based data structures are known to be computationally more efficient than their element-based counterparts (Luo *et al*, 1995).

2. MATHEMATICAL FORMULATION

In the two dimensional case the equation which defines an elliptic problem in a heterogeneous and anisotropic medium can be written as

$$\nabla \cdot \left(\underset{\sim}{K}\left(\vec{x}\right)\nabla u \right) = f\left(\vec{x}\right) \text{ with } \vec{x} = \left(x, y\right) \in \Omega \subset \mathbb{R}^2 \tag{1}$$

where,

$$\underset{\sim}{K}\left(\vec{x}\right) = \underset{\sim}{K} = \begin{pmatrix} K_{xx} & K_{xy} \\ K_{yx} & K_{yy} \end{pmatrix} \tag{2}$$

is a symmetric matrix that is allowed to be discontinuous through the internal boundaries of the domain Ω.

In order to formally define an elliptic problem (Crumpton, 1995), we further assume that

$$K_{xx}K_{yy} > K_{xy}^2 \tag{3}$$

Integrating Eq. (1) and applying the Green-Gauss theorem to its left side, yields

$$\int_{\Gamma} \left(\underset{\sim}{K}\nabla u \right) \cdot \vec{n}\partial\Gamma = \int_{\Omega} f \partial\Omega \tag{4}$$

Equation (4) which is the integral form of Eq. (1), defines, for instance, the pressure field for the fluid flow of oil and water in heterogeneous and anisotropic petroleum reservoirs or the transport of contaminants in aquifers (Rees *et al*, 2004; Carvalho *et al*, 2005).

3. NUMERICAL FORMULATION

As mentioned before, in the present work, we have adopted a vertex centered finite volume procedure with median dual control volumes built over a triangular primary mesh, in which the geometric coefficients necessary to our calculation are associated to the edges and to the nodes of the primary mesh (Luo *et al*, 1995; Crumpton *et al*, 1997; Sorensen, 2001; Rees *et al*, 2004; Carvalho *et al*, 2005). These edge and node coefficients are pre-computed in a pre-processing stage from the more traditional element data structure which is commonly used in the finite element method context.

For a general node *I* of the mesh, Eq. (4) can be approximated as:

$$\sum_{L_I} \vec{F}_{IJ_L}^{\Omega} \cdot \vec{C}_{IJ_L} + \sum_{L_I} \vec{F}_{IJ_L}^{\Gamma} \cdot \vec{D}_{IJ_L} = f_I V_I \tag{5}$$

where $\vec{F}_{IJ_L} = \underset{\sim}{K}\nabla u_{IJ_L}$ is the flux function defined at the control surface, V_I is the volume of the CV surrounding node *I*, the upper index Ω represents approximations that are associated to every edge IJ_L of the mesh which is connected to node *I*, Γ refers only to boundary edges connected to that node, and the summation $\sum_{L_I}$ is performed over the edges $\left(L_I\right)$ connected to node *I*. The geometrical coefficients $\vec{C}_{IJ_L}$ and $\vec{D}_{IJ_L}$ are defined as

$$\vec{C}_{IJ_L} = A_{K+1}\vec{n}_{K+1} + A_K\vec{n}_K$$
$$\vec{D}_{IJ_L} = A_L\vec{n}_L \tag{6}$$

In Equation (6), A_K, A_{K+1} and A_L are the areas of the control surfaces associated to the control surface normals $\vec{n}_K$, $\vec{n}_{K+1}$ and $\vec{n}_L$, respectively. Further details can be found in (Carvalho *et al*, 2005).

In order to approximate the mid-edge gradients/fluxes required in Eq. (5), different strategies can be devised (Svärd and Nordström, 2003). A classical approach involves using a simple two point approximation in which mid-edge fluxes are formally second order accurate only if the media is isotropic and the straight lines that connects two adjacent nodes and the control surfaces are orthogonal to each other, as in the case of the Voronoi tessellations (Edwards, 2000). Schemes using such approaches are equivalent to the so called control volume finite difference methods (CVFD).

In the present paper, we use a different approach which has been originally devised by Crumpton *et al* (1997) for the discretization of diffusion terms in the Navier-Stokes equations. In this approach, in order to obtain the final discrete system of equations, we first determine nodal gradients as functions of the discrete scalar field and then, we use these gradients to compute the elliptic terms in a second step (Crumpton *et al*, 1997; Sorensen, 2001) naturally arise when we are handling full tensor problems, i.e. $K_{xy} = K_{yx} \neq 0.0$ or when we are using non-orthogonal meshes, as both problems can be seen as equivalents (Edwards and Rogers, 1998).

In order to compute the nodal gradient, we make use of the Gauss-Green theorem to integrate the gradient of the scalar variable at node *I*, obtaining

$$\int_{\Omega_I} \nabla u_I \, \partial\Omega_I = \int_{\Gamma_I} u_I \vec{n} \, \partial\Gamma \tag{7}$$

Assuming that the average gradient in the control volume can be defined as

$$\nabla u_I V_I = \int_{\Omega_I} \nabla u_I \partial\Omega_I \tag{8}$$

Similarly to Eq. (5), we can write the discrete form of Eq. (7) as

$$\nabla u_I V_I = \left(\sum_{L_{I(\Omega)}} u^{\Omega}_{IJ_L} \vec{C}_{IJ_L} + \sum_{L_{I(\Gamma)}} u^{\Gamma}_{IJ_L} \vec{D}_{IJ_L} \right) \tag{9}$$

Further, we must adopt the following linear edge approximations

$$u^{\Omega}_{IJ_L} = \frac{u_I + u_{J_L}}{2} \quad \text{and} \quad u^{\Gamma}_{IJ_L} = \frac{5u_I + u_{J_L}}{6} \tag{10}$$

Inserting Eq. (10) in Eq. (9), we obtain

$$\nabla u_I = \frac{1}{V_I}\left[\sum_{L_{I(\Omega)}} \vec{C}_{IJ_L} \frac{\left(u_I + u_{J_L}\right)}{2} + \sum_{L_{I(\Gamma)}} \vec{D}_{IJ_L} \frac{\left(5u_I + u_{J_L}\right)}{6} \right] \tag{11}$$

The boundary term $\left(u^{\Gamma}_{IJ_L}\right)$ defined in Eq. (10) assumes a piecewise linear interpolation for boundary fluxes similar to a FEM type approximation, being formally second order accurate in space when linear triangles are used (Luo *et al*, 1995).

3.1. Anisotropic and heterogeneous media

In the case of heterogeneous media, fluxes definitions over the edges located at the interface between different materials can be ambiguous (Helming and Huber, 1998). If gradients computed as described in Eq. (11) are directly used for flux computations, an inconsistent flux would be obtained along CV faces adjacent to material discontinuities.

In order to circumvent this problem, gradients are recovered in a sub-domain by sub-domain approach. First, material properties (e.g. porosity and permeability) are associated to sub-domains. For each physical sub-domain, we store a list of edges and nodes and their associated geometrical coefficients. For the mesh considered in Fig. (1), it is necessary to include new geometrical coefficients, $\vec{D}_{IJ_L} = A_L \vec{n}_L$ and $\vec{D}_{IJ_M} = A_M \vec{n}_M$, which are quantities related to internal boundary edges, in order to correctly reconstruct gradients and fluxes in a particular sub-domain. These coefficients are used to obtain a second order recovery of gradients for each physical sub-domain of the problem, allowing for a discontinuous flux computation. Therefore, for heterogeneous media, we can rewrite Eq. (11) as

$$\nabla u_I^{\Omega_R} = \frac{1}{V_I^{\Omega_R}} \left[\sum_{L_{I(\Omega_R)}} \vec{C}_{IJ_L}^{\Omega_R} \frac{\left(u_I + u_{J_L}\right)}{2} + \sum_{L_{I(\Gamma_{RE})}} \vec{D}_{IJ_L}^{\Omega_R} \frac{\left(5u_I + u_{J_L}\right)}{6} + \sum_{L_{I(\Gamma_{RI})}} \vec{D}_{IJ_L}^{\Omega_R} \frac{\left(5u_I + u_{J_L}\right)}{6} \right] \tag{12}$$

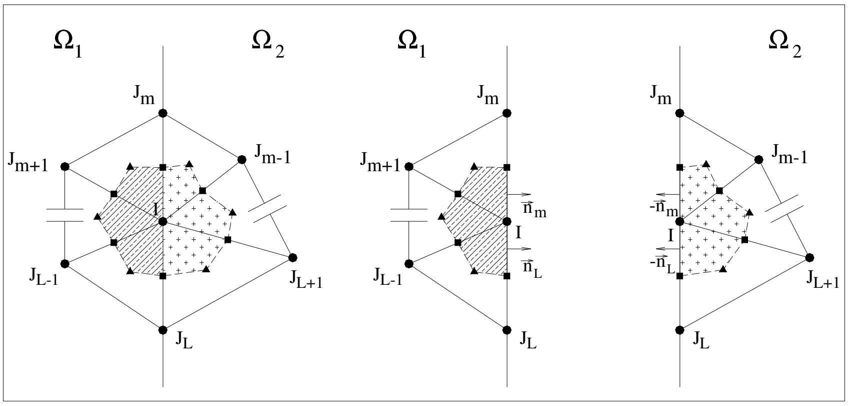

Figure 1. 2-D Control volume split by two different materials.

In Equation (12), $\nabla u_I^{\Omega_R}$ is the nodal gradient and $V_I^{\Omega_R}$ is the control volume of a node I associated to the sub-domain Ω_R, and $\vec{C}_{IJ_L}^{\Omega_R}$ and $\vec{D}_{IJ_L}^{\Omega_R}$ refer to the geometrical coefficients of the edge IJ_L associated to the same sub-domain Ω_R. Finally, note that in this sub-domain approach, $\vec{D}_{IJ_L}^{\Omega_R}$ refers to both, external and internal boundary edges, and Γ_{RE} and Γ_{RI} refer, respectively, to loops over external boundary edges and internal edges between multiple domains. In order to compute the fluxes of Eq. (5), we define a local frame of reference, in which one axis is placed along the edge direction (P), and another axis (N) is orthogonal to the direction (P), and subdivide the gradients into two components as stated in Eq. (13)

$$\nabla u_{IJ_L}^{\Omega_R} = \nabla u_{IJ_L}^{\Omega_R(N)} + \nabla u_{IJ_L}^{\Omega_R(P)} \tag{13}$$

The component of the gradient parallel to the edge direction $\nabla u_{IJ_L}^{\Omega_R(P)}$ is replaced by a local second order central difference approximation $\nabla u_{IJ_L}^{\Omega_R(P^*)}$, as follows

$$\nabla u_{IJ_L}^{\Omega_R *} = \nabla u_{IJ_L}^{\Omega_R(N)} + \nabla u_{IJ_L}^{\Omega_R(P^*)} \tag{14}$$

where:

$$\nabla u_{IJ_L}^{\Omega_R(P^*)} = \frac{\left(u_{J_L} - u_I\right)}{\left|\Delta_{IJ_L}\right|} \vec{L}_{IJ_L} \tag{15}$$

In Equation (15) $\left|\Delta_{IJ_L}\right|$ and $\vec{L}_{IJ_L} = \overline{IJ}_L \big/ \left|\Delta_{IJ_L}\right|$ are, respectively, the length and the unity vector of the edge IJ_L. From Equation (13), the normal component of the gradient associated to the edge IJ_L can be computed as

$$\nabla u_{IJ_L}^{\Omega_R(N)} = \nabla u_{IJ_L}^{\Omega_R} - \nabla u_{IJ_L}^{\Omega_R(P)} \tag{16}$$

where the gradient along the edge direction is given by

$$\nabla u_{IJ_L}^{\Omega_R(P)} = \left(\nabla u_{IJ_L}^{\Omega_R} \cdot \vec{L}_{IJ_L}\right)\vec{L}_{IJ_L} \tag{17}$$

with

$$\nabla u_{IJ_L}^{\Omega_R} = \frac{\nabla u_I^{\Omega_R} + \nabla u_{J_L}^{\Omega_R}}{2} \tag{18}$$

Inserting Eq. (17) in Eq. (16) yields

$$\nabla u_{IJ_L}^{\Omega_R(N)} = \nabla u_{IJ_L}^{\Omega_R} - \left(\nabla u_{IJ_L}^{\Omega_R} \cdot \vec{L}_{IJ_L}\right)\vec{L}_{IJ_L} \tag{19}$$

Inserting Eq. (15) and Eq. (19) in Eq. (14), we have

$$\nabla u_{IJ_L}^{\Omega_R *} = \nabla u_{IJ_L}^{\Omega_R} - \left(\nabla u_{IJ_L}^{\Omega_R} \cdot \vec{L}_{IJ_L}\right)\vec{L}_{IJ_L} + \frac{\left(u_{J_L} - u_I\right)}{\left|\Delta_{IJ_L}\right|}\vec{L}_{IJ_L} \tag{20}$$

Defining the continuous "hybrid" mid-edge flux function as

$$F_{IJ_L}^{\Omega_R *} = -\underset{\sim}{K}^{\Omega_R}\nabla u_{IJ_L}^{\Omega_R *} \tag{21}$$

in which the term hybrid was used to indicate that one part of the mid-edge gradient/flux (i.e. the cross-diffusion term) is computed using the traditional edge-based finite volume approach by averaging the nodal Green-Gauss gradients, and the other part is computed using the compact two point finite difference scheme.
Inserting Eq. (20) in Eq. (21), we can write

$$\vec{F}_{IJ_L}^{\Omega_R *} = -\underset{\sim}{K}^{\Omega_R}\left(\nabla u_{IJ_L}^{\Omega_R} - \left(\nabla u_{IJ_L}^{\Omega_R} \cdot \vec{L}_{IJ_L}\right)\vec{L}_{IJ_L} + \frac{\left(u_{J_L} - u_I\right)}{\left|\Delta_{IJ_L}\right|}\vec{L}_{IJ_L}\right) \tag{22}$$

Using Eq. (18) in Eq. (22), we can redefine Eq. (5) using this new surface flux approximation as

$$\sum_{R=1}^{Ndom}\left(\sum_{L_{I(\Omega_R)}} \vec{F}_{IJ_L}^{\Omega_R *} \cdot \vec{C}_{IJ_L}^{\Omega_R} + \sum_{L_{I(\Gamma_R)}} \vec{F}_{IJ_L}^{\Gamma} \cdot \vec{D}_{IJ_L}^{\Omega_R}\right) = \sum_{R=1}^{Ndom} f_I^{\Omega_R} V_I^{\Omega_R} \tag{23}$$

In the equation above, $\vec{F}_{IJ_L}^{\Gamma} \cdot \vec{D}_{IJ_L}^{\Omega_R}$ must be replaced by the appropriate Neumann boundary condition and *Ndom* refers to the number of domains that surrounds node *I*.

It must be emphasized that, while source terms are simply volume averaged quantities, nodal gradients and fluxes are recovered in a sub-domain by sub-domain basis (i.e. looping over sub-domains) in order to formally guarantee that both are correctly approximated for each material along interface edges. This approach produces, in general, a non-symmetric system of equations that is assembled in a sub-domain approach and has been solved using a simple sparse Gauss elimination solver.

the expression above is built in

4. ERROR EVALUATION

In order to evaluate the errors in the example to be presented, we define the asymptotic truncate error as

$$\left\|E_h\right\| = Ch^q + O\left(h^{q+1}\right) \tag{24}$$

In Equation (24), h is the mesh spacing, q is the order of the error, C is a constant independent of h and $\|\cdot\|$ refers to some specified norm. The numerical convergence rate is estimated as

$$q \cong \log_2 \frac{\|E_h\|}{\|E_{h/2}\|} \tag{25}$$

Following Crumpton (1995), we define the root mean square error as

$$\|E\|_{RMS} = \|\hat{u} - u\|_{L_{RMS}} = \left(\sum_{I=1}^{NP} (\hat{u} - u)^2 \Big/ NP \right)^{1/2} \tag{26}$$

where u is the exact solution, $\hat{u}$ is the approximate solution and NP is the number of nodes of the mesh.

5. EXAMPLE: DISCONTINUOUS AND ANISOTROPIC MEDIA

In order to evaluate and compare the accuracy of the proposed finite volume procedure for the solution of elliptic equations with discontinuous and anisotropic coefficients and discontinuous distributed source terms, we present the results obtained for a benchmark problem which was originally presented in Crumpton (1995) that solved this problem using a flux continuous finite volume scheme using structured orthogonal quadrilateral meshes. In this problem, defined by Eq. (1), we consider a unity square domain (i.e. $[-1,1]\mathrm{X}[-1,1]$) with numerical boundary conditions obtained from the exact solution, which is also valid at domain boundaries. The discontinuous source term and the full tensor discontinuous diffusion coefficients are given by

$$f(x,y) = \begin{cases} \left[-2sin(y) - \cos(y)\right]\alpha x - sin(y) & \text{for} \quad x \le 0 \\ 2\alpha \exp(x)\cos(y) & \text{for} \quad x > 0 \end{cases} \tag{27}$$

$$\underset{\sim}{K} = \begin{cases} \begin{pmatrix} 1 & 0 \\ 0 & 1 \end{pmatrix} & \text{for} \quad x < 0 \\ \alpha \begin{pmatrix} 2 & 1 \\ 1 & 2 \end{pmatrix} & \text{for} \quad x > 0 \end{cases} \tag{28}$$

where α is the intensity of the discontinuity between the two different regions. The exact solution for this problem is given by Crumpton (1995) as

$$u(x,y) = \begin{cases} \left[2sin(y) + \cos(y)\right]\alpha x + sin(y) & \text{for} \quad x \le 0 \\ \exp(x)\cos(y) & \text{for} \quad x > 0 \end{cases} \tag{29}$$

We have solved this problem for using a sequence of uniform unstructured triangular meshes that were directly generated over the computational domain with a mesh spacing in such a way that the triangular meshes had approximately $(8\mathrm{x}8)$, $(16\mathrm{x}16)$, $(32\mathrm{x}32)$ e $(64\mathrm{x}64)$ elements. Figures (2.a) to (2.d) present the iso-contours for the scalar function $u(x,y)$ obtained by the EBFV with the $(64\mathrm{x}64)$ mesh associated to $\alpha = 1.0$; (b) $\alpha = 10.0$; (c) $\alpha = 100.0$; (d) $\alpha = 1000.0$, respectively.

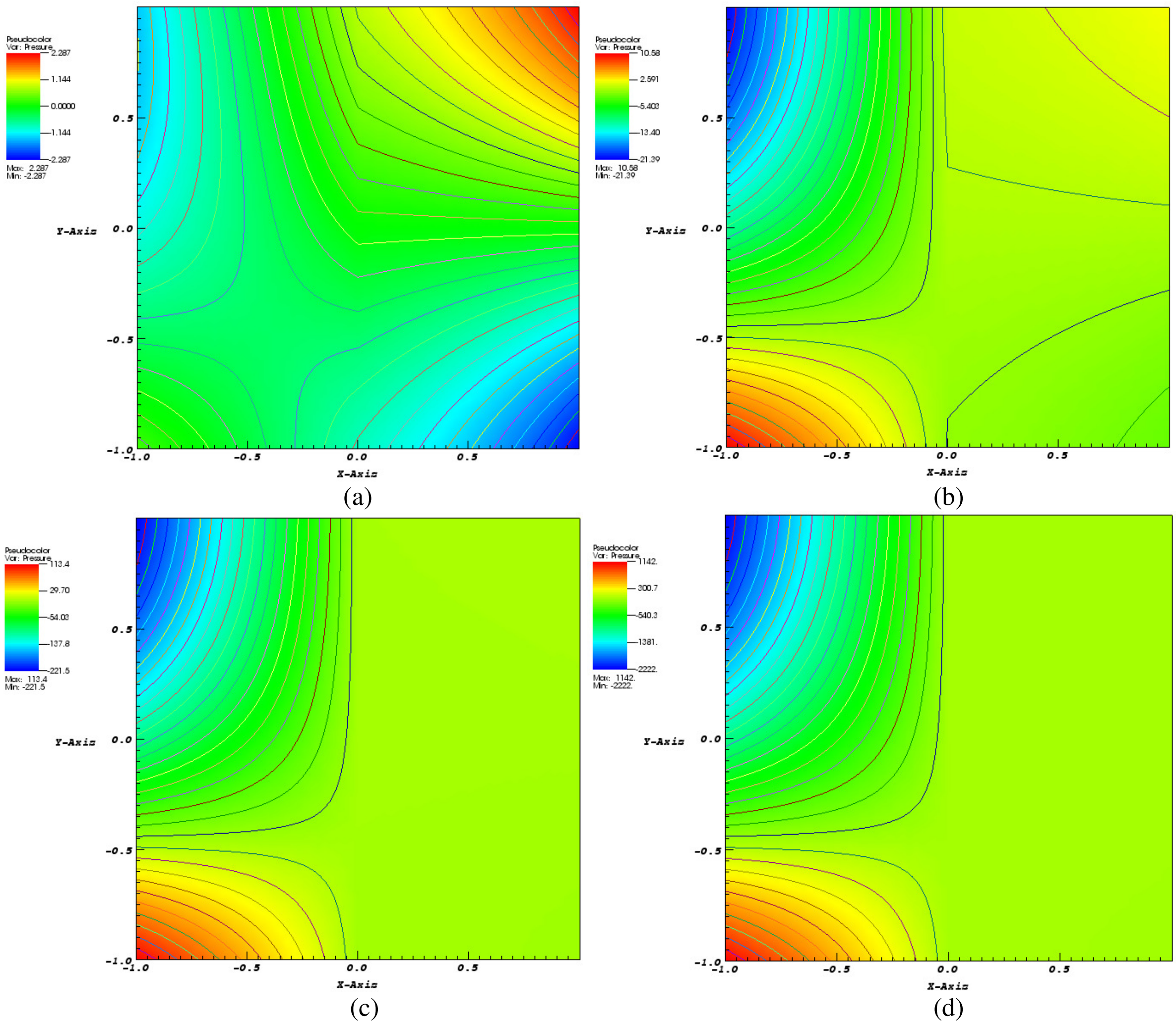

Figure 2. Iso-contours of the scalar function $u(x, y)$ obtained with unstructured triangular mesh $(64\text{x}64)$ for the different values of α : (a) $\alpha = 1.0$; (b) $\alpha = 10.0$; (c) $\alpha = 100.0$; (d) $\alpha = 1000.0$.

Tables (1), (2), (3) and (4) present the root mean square errors, $\|E\|_{RMS}$, and the convergence rates q_{RMS}, for the four different values of (a) $\alpha = 1.0$; (b) $\alpha = 10.0$; (c) $\alpha = 100.0$; (d) $\alpha = 1000.0$, obtained with our edge-based finite volume formulation (EBFV) and with the flux continuous finite volume method of Crumpton (CFV). As it can be clearly observed in Tab. (1), (2), (3) and (4), the EBFV presents second order accuracy for all values of α. From Tables (1) to (4) we can note that the increase of the strength of the discontinuity also increase the magnitude of the error for both, the EBFV and the Crumpton's CFV schemes, even though the EBFV presents slightly better results for this particular problem. It is also clear that, independently of the strength of the discontinuity, the EBFV and the Crumpton's CFV are both second order accurate.

Table 1. Errors and convergence rates for $\alpha = 1.0$.

Mesh Divisions N	$\|E\|_{RMS}$ (EBFV)	$\|E\|_{RMS}$ (CFV)	q_{RMS} (EBFV)	q_{RMS} (CFV)
8	3.4e-003	3.33e-003	-----------	-----------
16	6.70e-004	9.37e-004	2.2683	1.8294
32	1.49e-004	2.45e-004	2.1149	1.9353
64	3.33e-005	6.25e-005	2.1383	1.9709

Table 2. Errors and convergence rates for $\alpha = 10.0$.

Mesh Divisions N	$\|E\|_{RMS}$ (EBFV)	$\|E\|_{RMS}$ (CFV)	q_{RMS} (EBFV)	q_{RMS} (CFV)
8	5.60e-003	1.64e-002	-----------	-----------
16	1.00e-003	4.35e-003	2.4501	1.9146
32	2.10e-004	1.11e-003	2.3066	1.9705
64	4.25e-005	2.81e-004	2.3083	1.9819

Table 3. Errors and convergence rates for $\alpha = 100.0$.

Mesh Divisions N	$\|E\|_{RMS}$ (EBFV)	$\|E\|_{RMS}$ (CFV)	q_{RMS} (EBFV)	q_{RMS} (CFV)
8	4.38e-002	1.81e-002	----------	----------
16	8.40e-003	4.74e-003	2.3710	1.9330
32	1.40 e-003	1.21e-003	2.5866	1.9699
64	2.44e-004	3.04e-004	2.5279	1.9929

Table 4. Errors and convergence rates for $\alpha = 1000.0$.

Mesh Divisions N	$\|E\|_{RMS}$ (EBFV)	$\|E\|_{RMS}$ (CFV)	q_{RMS} (EBFV)	q_{RMS} (CFV)
8	4.38e-001	1.83e-000	----------	----------
16	8.54e-002	4.79e-001	2.3580	1.9337
32	1.40e-002	1.22e-001	2.6030	1.9731
64	2.40 e-003	3.07e-002	2.5251	1.9906

6. CONCLUSIONS

In the present paper we have described an edge-based node centered finite volume formulation (EBFV) which was used to solve elliptic type equations with highly discontinuous coefficients very accurately. Full tensors and flexible (unstructured) non-orthogonal triangular meshes are treated naturally in our formulation. In order to show the potential of the presented finite volume procedure we have solved a benchmark problem that involves full tensor and highly discontinuous diffusion coefficients and discontinuous distributed source terms. Our results (not fully presented here) are quite promising and compare very favorably with other results found in literature.

7. ACKNOWLEDGEMENTS

The authors would like thank the National Research Council (CNPQ) and the National Petroleum Agency (ANP) for the financial support.

8. REFERENCES

Aavatsmark, I., Barkve, T., Bøe, Ø., Mannseth, T., 1998, "Discretization on Unstructured Grids for Inhomogeneous, Anisotropic Media. Part I: Derivation of the Methods", Siam J. Sci. Comput. Vol. 19, pp. 1700-1716.

Carvalho, D.K.E., Lyra, P.R.M., Willmersdorf, R.B., Araújo, F.D.S., 2005, "An Unstructured Edge-Based Finite Volume Formulation for Solving Immiscible Two-Phase Flows in Porous Media. Communications in Numerical Methods in Engineering, Vol. 21, pp. 747-756.

Crumpton, P.I., 1995, "Discretization and Multigrid Solution of Elliptic Equations with Mixed Derivative Terms and Strongly Discontinuous Coefficients", Journal of Computational Physics, Vol. 116, pp. 343-358.

Crumpton, P.I., Moinier P., Giles, M.B.T.J., 1997, "An Unstructured Algorithm for High Reynolds Number Flows on Highly Stretched Grids", In: Numerical Methods in Laminar and Turbulent Flow, Taylor C, Cross J.T. (Eds). Pineridge Press: Swansea, pp. 561–572.

Edwards, M.G., Rogers, C.F., 1998, "Finite Volume Discretization with Imposed Flux Continuity for the General Tensor Pressure Equation", Computational Geosciences 2, Vol. 2, pp. 259-290.

Edwards, M.G., 2000, "M-Matrix Flux Splitting for General Full Tensor Discretization Operators on Structured and Unstructured Grids", Journal of Computational Physics, Vol. 160, pp. 1-28.

Ewing, R.E., 1983, "The Mathematics of Reservoir Simulation", Siam, Philadelphia.

Klausen R. A., Eigestad, G. T., 2004, "Multi-Point Flux Approximations and Finite Element Methods: Practical Aspects of Discontinuous Media", 9th European Conference on the Mathematics of Oil Recovery. Cannes, France

Helmig R, Huber R., 1998, "Comparison of Galerkin-type discretization techniques for two-phase flow problems in heterogeneous porous media". Advances in Water Resources, Vol. 21, pp. 697-711.

Loula, A.F.D., Garcia, E.L.M., Coutinho, A.L.G.A., 1999, "Miscible displacement simulation by finite element methods in distributed memory machines", Computer Methods in Applied Mechanics, Vol. 174, pp. 339-354.

Luo, H., Baum, J.D., Löhner, R., 1995, "An Improved Finite Volume Scheme for Compressible Flows on Unstructured Grids", Technical Report, AIAA Paper, pp. 95-0348.

Rees, I., Masters, I., Malan, A.G., Lewis, R.W., 2004, "An Edge-Based Finite Volume Scheme for Saturated-Unsaturated Groundwater Flow", Computer Methods in Applied Mechanics, Vol. 193, pp. 4741-4759.

Sorensen, K.A., 2001, "A Multigrid Accelerated Procedure for the Solution of Compressible Fluid Flows on Unstructured Meshes", Department of Civil Engineering – University Of Wales/Swansea- Uk, Ph.D. Thesis C/Ph/161/01.

Svärd, M, Nordström, J., 2003, "A stable and accurate summation by parts finite volume formulation of the laplacian operator". Uppsala Universitet, Institutionen för Informationsteknologi, Technical Report 003, pp. 1-36.

9. RESPONSIBILITY NOTICE

The authors are the only responsible for the printed material included in this paper.